Peer-reviewed version available at Gels 2018, 4, 35; doi:10.3390/gels4020035

*Review*

# Hybrid Physical Gels from Polymers and Self-Assembled Systems: A Novel Path for Making Functional Materials

**Jean-Michel Guenet** [1]

[1] Institut Charles Sadron, CNRS-Université de Strasbourg, 23 rue du Loess, BP 84047, 67034 STRASBOURG Cedex2, France;

* Correspondence: jean-michel.guenet@ics-cnrs.unistra.fr; Tel.: +33-388-41-41-45

**Abstract:** The synthesis these past few years of novel organic molecules that spontaneously self-assemble into a large variety of molecular architecture, particularly generating organogels, has opened up new horizons for preparing functional materials. Here, we present an original preparation path of such materials through the making of hybrid gels of these molecules together with covalent polymers. Three types of systems are described: i) intermingled gels where a polymer gel and an organogel pervade one another; ii) encapsulation of self-assembled filaments in polymer fibrils, which provides a system with unusual magnetic properties; iii) the reverse situation where self-assembled nanotubes sheathe polymer fibrils. Here two covalent polymers are considered: a neutral polymer, namely stereoregular polystyrene (isotactic or syndiotactic), and a semi-conducting polymer, P3BT. In the latter case, semi-conducting nanowires are obtained.

**Keywords:** polymer thermoreversible gels; self-assembled systems; functional materials.

## 1. Introduction

The past two decades have witnessed the thriving of new organic molecules capable of self-assembling that, once in solution, subsequently generate a large variety of molecular architectures such as filaments, fibrils, platelets, and the like [1-6]. In many cases the resulting macroscopic state consists of a gel-like or a paste-like substance. Interestingly, some of these molecules further possess functional properties [2] (magnetic, opto-electronic, electronic, and s.o...) that can open new horizons for developing functional materials in replacement for and/or in addition to current natural compounds (for instance, the replacement of rare earths would be a tremendous achievement). Yet, in many cases, these systems cannot be processed into functional materials for various reasons, such as their limited amount due to their complex syntheses, and correspondingly their cost, and/or their poor mechanical properties due to use of low concentrations.

As a rule, a functional material is rarely obtained from a pure compound. The best example is provided by metallic alloys whose properties depend upon the subtle mixture of different metals. In the realm of polymers one can quote rubber-made car tyres that also contain carbon black and/or silica with the aim of reducing their wear. Also, a new property, foreign to the basic constituents, may be eventually imparted to the resulting material.

Among self-assembling systems some are often designated as supramolecular polymers [7] since they form thread-like objects (filaments or fibrils) as covalent polymers do. Mixing these self-assembling systems with covalent polymers seems to be a straightforward way of preparing hybrid materials.

Here, we review a new approach consisting in preparing hybrid gels where the main component is a thermally reversible polymer gel wherein the self-assembled system is imbedded. Polymer thermoreversible gels are fibrillar networks with a typical mesh size in the micron range [8]. As far as morphology is concerned they resemble to a very high extent organogels, namely array of fibrils of similar mesh size. The idea is basically to use the polymer as a matrix, which can lower the

Peer-reviewed version available at Gels 2018, 4, 35; doi:10.3390/gels4020035



cost of the material, enhance the mechanical properties of the hybrid system, and make the tractability much easier [6]. That the hybrid gel contains a large amount of solvent does not stand as a major problem since it can be dried in many ways (simple evaporation, CO2 critical extraction,…). The solvent can also be recycled as is the case with the making of the PVC fibres (Rhovyl) [9]. Supercritical CO2 extraction can be a good choice as it allows one to keep the original morphology of the hybrid network.

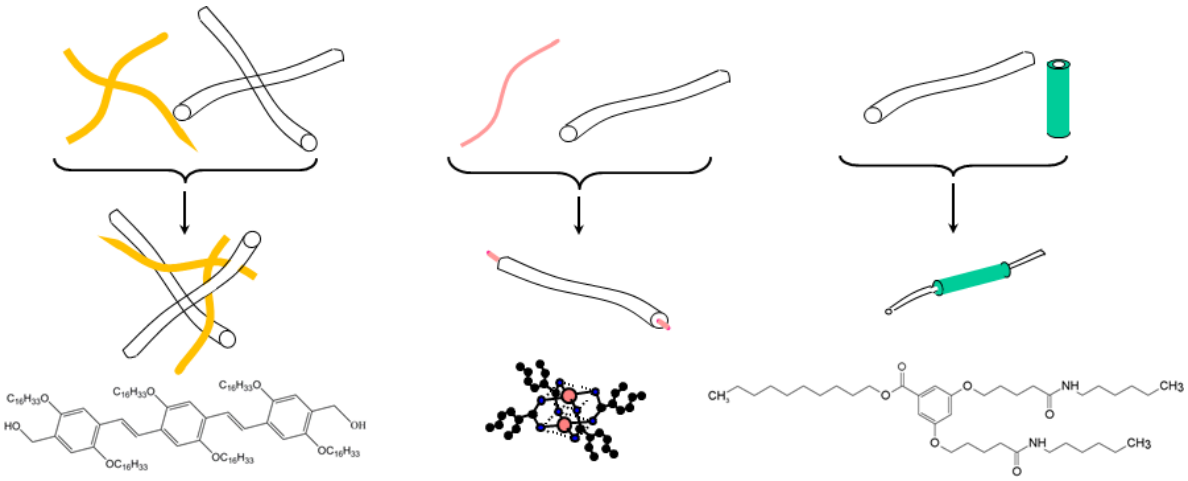

**Figure 1.** The three types of hybrid materials: left: an intermingled hybrid gel polymer gel with the organogelator shown underneath (designated as OPVOH, yellow); middle: encapsulation of a self-assembled filaments of a bicopper complex molecule shown underneath (pink) designated as CuS8;; ●= copper, ●= oxygen; ●= carbon) into a polymer fibril; right a self-assembled nanotube (green), molecule shown underneath, designated as BHPB-10, sheathing a polymer fibril.

In this review we will present three types of hybrid materials with different ways of using the polymer matrix as portrayed in figure 1. The first case consists of preparing an ***intermingled gel*** where gels pervade one another. In the second case, ***polymer fibrils encapsulate filaments*** of a self-assembled bicopper complex. The third case is the reverse situation where ***self-assembled nanotubes sheathe polymer fibrils***. In the last two cases, heterogeneous nucleation is the driving process.

## 2. Results and Discussion

### *2.1. Preparing interminghled gels*

In this section, the feasibility of intermingling a polymer thermoreversible gel together with an organogel, the latter bearing an opto-electronic function, is shown and discussed. The polymer gels are made up of either isotactic polystyrene (iPS) or syndiotactic polystyrene (sPS). The organogelator is an oligo phenylene vinylene (OPVOH, see figure 1) which possesses opto-electronic properties, the remarkable aspect being a change of colour at the SOL-GEL transition [2]. In most cases two covalent polymers cannot be mixed on account of entropic grounds. The question to be addressed in the case of covalent polymers and supramolecular polymers concerns therefore their degree of compatibility. In other words can one prepare homogeneous solutions at high temperature that will further gel upon cooling without triggering first a liquid-liquid demixtion? In this aim, a mixture of OPVOH and atactic polystyrene (aPS) has been dissolved in benzene by heating ($C_{OPV}$= 0.004 g/cm$^3$, $C_{aPS}$= 0.04 g/cm$^3$), and then subsequently cooled down to form the organogel (aPS does not gel under these conditions). As displayed in figure 2, the formation and melting behaviour of the organogel is not affected by the presence of atactic polystyrene. AFM images also confirm that the gel morphology has not be significanly altered by the polymer chains [10].

The preparation of polymer/OPVOH intermingled networks has therefore been achieved with

Preprints (www.preprints.org) | NOT PEER-REVIEWED | Posted: 22 March 2018 doi:10.20944/preprints201803.0193.v1

Peer-reviewed version available at Gels 2018, 4, 35; doi:10.3390/gels4020035



either type of stereoregular polystyrene (iPS or sPS) on account of their differing gelation behaviour [8]. They form in different solvents, and they grow and melt at different temperatures.

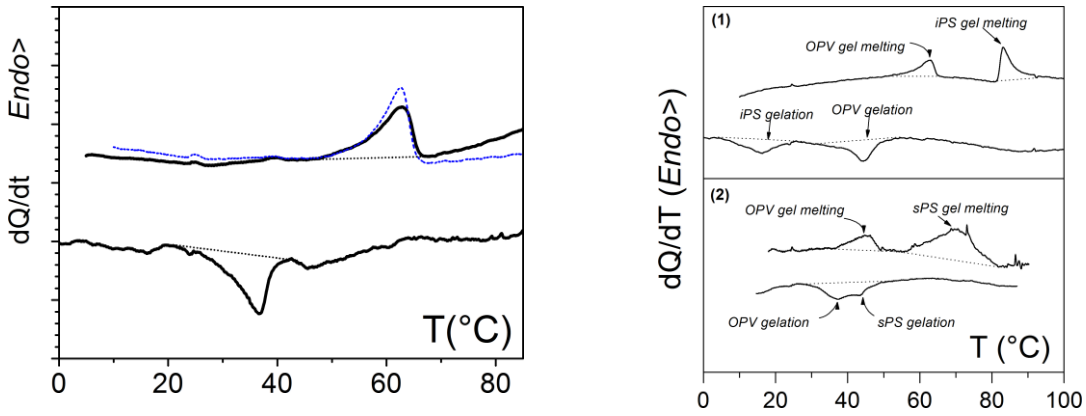


(**a**) (**b**)

**Figure 2.** DSC thermograms; (a): the OPVOH organogel formation and melting, in blue the gel melting in the ternary system OPVOH/aPS/benzene, where $C_{aPS}$= 2.5x10$^{-2}$ g/cm$^3$ and $C_{OPVOH}$= 0.4x10$^{-2}$ g/cm$^3$; (b) ternary gels: (1) isotactic polystyrene/OPVOH in *trans*-decahydronaphthalene; (2) syndiotactic polystyrene/OPVOH in benzene, where $C_{polymer}$= 7x10$^{-2}$ g/cm$^3$ and $C_{OPVOH}$= 0.4x10$^{-2}$ g/cm$^3$ (data from Dasgupta et al. [10]). For details see text.

Typical DSC traces are shown in figure 2. Again, the presence of a foreign molecule does not perturb the gelation of the other component. The formation and melting temperatures are virtually identical, within experimental uncertainties, to those observed in binary systems. Further SAXS experiments not shown here reveal that the scattering by the ternary system is simply the sum of the scattering by each binary gels. AFM together with SEM investigations presented in figure 3 [10] clearly point out that the gels pervade one another. Note that the the cross-sections of the organogel fibrils are much thicker than those of the polymer gel.

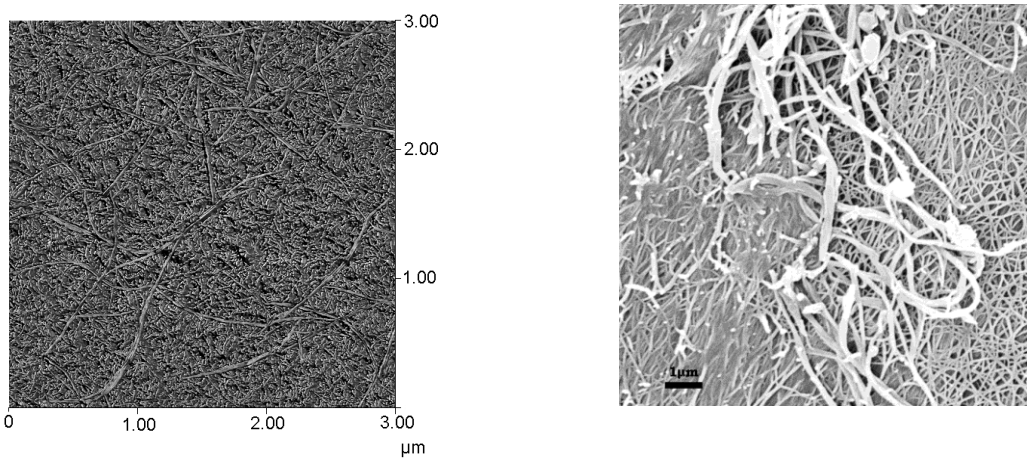


(**a**) (**b**)

**Figure 3.** (a) AFM picture of an sPS/OPVOH gel in benzene [10]. (b): SEM picture of aa sPS/OPVOH gel in p-xylene (courtesy of Christophe Daniel, Universita di Salerno, Italy). In both cases the fibrils of largest cross-sections are those from the organogel (typically ~ 200 nm against ~ 60nm).

As aforementioned, OPVOH systems change colour at the SOL-GEL transition. This stems from π-π interactions that establish during the gelation process [2]. In the hybrid gel sPS/OPVOH/toluene, the change of colour is again observed, yet without macroscopic melting (figure 4). DSC data in figure 2B account readily for this effect: as long as the temperature is kept below the polymer gel

Peer-reviewed version available at Gels 2018, 4, 35; doi:10.3390/gels4020035



melting, the OPVOH organogel moiety will repeatedly undergo a change of colour at its GEL-SOL-GEL transitions [10].

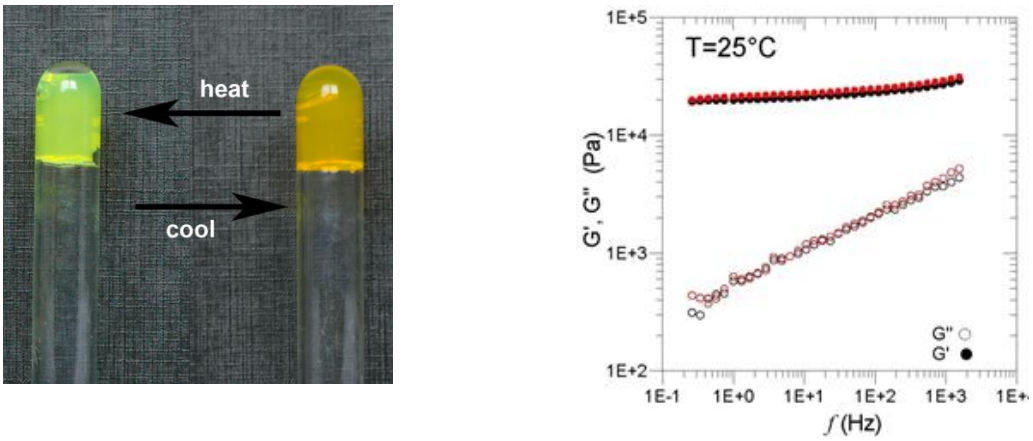


(**a**) (**b**)

**Figure 4.** (a) change of colour of the hybrid gel upon heating and cooling cycles. As long as temperature lies below the polymer gel melting point, the hybrid system remains a macroscopic gel [10]. (b) rheological properties of the hybrid gel (●) versus those of the binary sPS gel (●) the solvent is trans-decahydronaphthalene (unpublished data J.M. Guenet, D. Collin [11], Institut Charles Sadron).

Rheological experiments carried out by means of a piezzorheometer confirm that the mechanical properties are essentially those of the polymer gel. The values and the behaviour of both G′ and G′′ of the hybrid gel correspond within experimental uncertainties to those of the polymer gel [11].

The proof of concept is thus demonstrated: intermingled gels from covalent polymer gels and organogels can be prepared thanks to the high compatibility between their components. A functional property is therefore imparted to the polymer matrix with a low amount of organogelator, namely in a w/w ratio polymer/organogelator of about 20.

### *2.2. Encapsulating self-assembled filaments in polymer fibrils*

The bicopper complex molecule shown in figures 1 and 5 possesses the propensity of self-assembling in organic solvent, thus generating very long filaments containing only one molecule in their cross-section [12-13]. The filaments are typical supramolecular polymer but, due to the interaction of the order ok kT between molecules, are also designated as dynamic polymers since they break and reassemble with the tips of other filaments. The rheological behaviour of their organic solution is basically that of long covalent polymer chains and is well theroretically reproduced by means of a Maxwell model [13]. Filaments are stable over rather long times but 1D filaments gradually disappear to transform into a solid mesophase that eventually macroscopically phase separates.

The bicopper molecule possesses antiferromagnetic properties in the bulk state that are well described by the so-called Bleaney-Bowers relation [14,15]:

$$\chi_{CuS8} = \frac{N_A.g^2.\mu_B^2}{K_BT\left[3+exp\left(\frac{-2J}{K_BT}\right)\right]} \quad (1)$$

where NA is Avogadro's number, g the electron spin factor of the bicopper, J the coupling constant, $\mu_B$ Bohr's magneton.

That relation 1 fits the experimental results particularly means that bicopper molecules are magnetically behaving as if they were isolated (spin gap). The small upturn at very low T is usually due to paramagnetic impurities.

Abied et al. have shown that the molecular piling occurs through one copper atom interacting with the oxygen atom of its neighbour [16]. No intermolecular Cu-Cu interactions are therefore involved in the bulk state.

Although the 1-D aspect of the filaments might be of interest for testing their magnetic properties, their instability with time together with the impossibility of keeping them apart after solvent removal made this a remote option. The encapsulation of these filaments into polymer fibrils was contemplated by Lopez and Guenet thanks to existence of a common solvent a solvent, decahydronaphthalene, where the bicopper complex piles up into 1-D filaments while isotactic polystyrene forms a thermoreversible gel . [17]. It has been shown that the bicopper complex and the polymer form homogeneous solutions at high temperature, and are compatible to a large extent at lower temperature [18, 19].

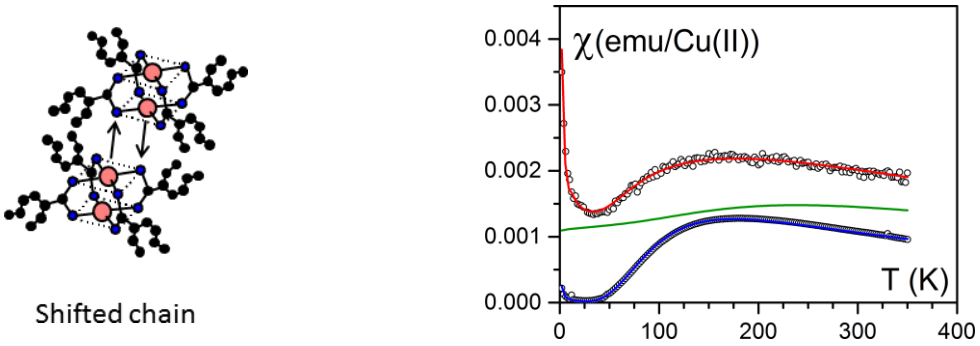


(**a**) (**b**)

**Figure 5.** (a) how bicopper molecules pile up in the bulk state (shifted chains) [12]. (b) magnetic susceptibility as a function of temperature. Blue= bulk state fitted with a Bleaney-Bowers law red= encapsulated state fitted by relation (1) (see text) [14,22], green theoretical variation for a spin chain [20].

Encapsulation the bicopper filaments into the polymer fibrils makes use of a *heterogeneous nucleation* process. The filaments that form first have been shown to act as an impurity towards the polymer, and so trigger the growth of the fibrils. Otherwise, polymer gel formation is driven by a *homogeneous nucleation* process. A heterogeneous nucleation mechanism implies that the impurity, namely the filaments, are located in the central core of the fibrils. DSC experiments have confirmed the occurrence of heterogeneous nucleation [17,20] by revealing the increase of the gel formation temperature while increasing the bicopper complex content.

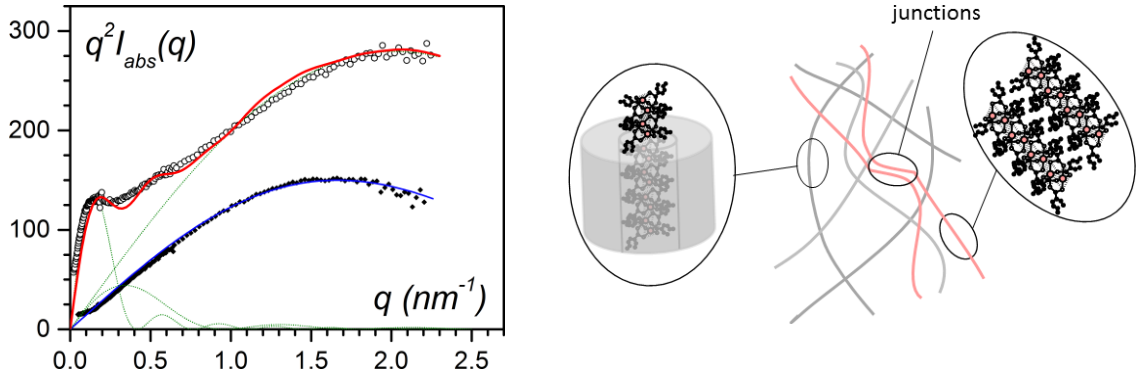


(**a**) (**b**)

**Figure 6.** (a) Small-angle neutron scattering data for IPS/CuS8/*trans*-decahydronaphthalene gels: in all cases $C_{IPS}$ = 0.04 g/cm³, ● for $C_{CuS8}$ = 0.038 g/cm³, ○ for $C_{CuS8}$ = 0.055 g/cm³. The solid lines (red and blue) are fit with theoretical models (see text for details) [17,20]. (b) sketch of the molecular structures for $C_{CuS8}$ = 0.055 g/cm³: encapsulated fibrils, free associated filaments and their junctions. The encapsulated fibrils represent 99% of the structures.

Preprints (www.preprints.org) | NOT PEER-REVIEWED | Posted: 22 March 2018 doi:10.20944/preprints201803.0193.v1

Peer-reviewed version available at Gels 2018, 4, 35; doi:10.3390/gels4020035



Small-angle neutron scattering experiments have allowed one to determine the structure of either the polymer or the bicopper complex by a proper matching contrast approach. These investigations show that the average polymer fibril cross-section decreases with increasing the bicopper content [21], an outcome in agreement with a heterogeneous nucleation process, but also that the central part of the fibrils consists of a different constituent, namely the bicopper complex. They further show that the filament structure is kept (figure 6) since for CuS8 concentrations below $C_{CuS8}$ = 0.04 g/cm³ the scattering curve can be fitted with a simple solid cylinder model:

$$q^2 I_{abs}(q) = 4\pi q C_{CuS8} \mu_{fil} \times \frac{J_1^2(qr_{fil})}{q^2 r_{fil}^2} \quad (2)$$

where $\mu_{fil}$ and $r_{fil}$ are the mass per unit length and the cross-sectional radius of the filaments, respectively, and $J_1$ the Bessel function of first kind and first order.

The fit of the experimental data yields $\mu_{fil}$= 1300 ± 100 g·mol$^{-1}$·nm$^{-1}$ and $r_{fil}$= 0.7 ± 0.1 nm, which confirms the near 1-D structure of the encapsulated filaments [20].

By increasing the bicopper complex content, part of the filaments are no longer encapsulated. Figure 6b shows the additional scattering due to the presence of associated 1-D filaments and to their sporadic junctions. The scattering curve can be then fitted with those three types of structures:

$$q^2 I_{abs}(q) = 4\pi q C_{CuS8} \left[ X\mu_{fil} \times \frac{J_1^2(qr_{fil})}{q^2 r_{fil}^2} + Y\mu_{fib} \times \frac{J_1^2(qr_{fib})}{q^2 r_{fib}^2} + Z\mu_{junc} \times \frac{J_1^2(qr_{junc})}{q^2 r_{junc}^2} \right] \quad (3)$$

where μ and r stand with appropriate subscripts for the mass per unit length and for the cross-sectional radius of the encapsulated filaments, the associated filaments and the junctions. X, Y, Z are the fractions of each species.

The fit yields $r_{fil}$= 0.67 nm, $r_{fil}$= 4 nm, and $r_{junc}$= 10 nm, $\mu_{fil}$= 1300 g/mol.nm,· $\mu_{fib}$= 7500 g/mol.nm and $\mu_{junc}$= 46 800 g/mol.nm, and X = 0.95, Y = 0.03, and Z = 0.02 [20].

As shown in figure 5 the magneric behaviour differs dratically whether the bicopper complex is in the bulk state or encapsulated. It was suspected that the piling of the molecules in the encapsulated filaments may differ from that in the bulk state [22]. To settle this point, Boulaoued et al. [20] have performed EXAFS (Extended X-Ray Absorption Fine Structure [23]) experiments for determining the environment of the copper atoms. While the model put forward by Abied et al. for the bulk state is confirmed [16], the experimental results conspicuously differ in the encapsulated state. It is concluded that Cu-0 interactions between adjecent molecules are replaced to a certain extent by Cu-Cu interactions (figure 7a). Thus, the encapsulated filaments are no longer purely shifted chains (figure 5a) but certainly contain spin chains (figure 7b).

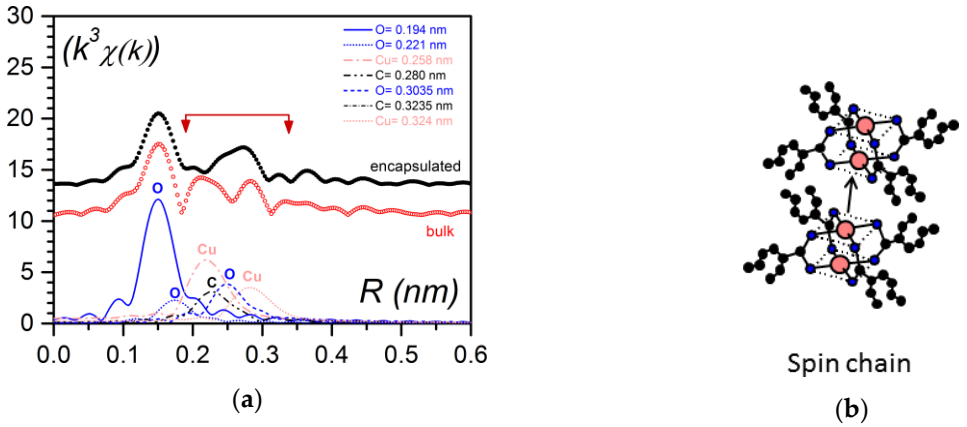


**Figure 7.** (a) Pseudo-radial distribution function in the vicinity of copper atoms as obtained by EXAFS; ● for the encapsulated bicopper complex, O for the bulk state (note there always is a difference of about 0.05 nm in EXAFS with the actual distances). The difference between the curves lies in the domain involving Cu-Cu distances (b) a spin chain where there Cu-Cu interaction between adjacent molecules occur in lieu of the Cu-O interaction seen in the bulk state [20,22].

Preprints (www.preprints.org) | NOT PEER-REVIEWED | Posted: 22 March 2018 doi:10.20944/preprints201803.0193.v1

Peer-reviewed version available at Gels 2018, 4, 35; doi:10.3390/gels4020035



From these conclusions, Boulaoued et al. have been able to fit their SQUID data by using a model where three species are contemplated: (i) a bicopper molecules with only intramolecular coupling (spin gap due to shifted chains) with $2J_{intra}$ the coupling constant. (ii) Antiferromagnetic spin chains with $2J_{intra}$ and $2J_{inter}$, namely inter and intra coupling constants. The alternation parameter $\alpha = 2J_{inter}/2J_{intra}$ is equal to 1 in case of a spin chain (gapless spin), and amounts to $\alpha$=0 for non-coupled dimers (shifted chains, spin gapped); iii) paramagnetic impurities. The magnetic susceptibility is then written:

$$\chi_{hybrid}=x\chi_{spingap}+y\chi_{gapless}+z\chi_{pm} \quad (4)$$

with obvious meaning as to the subscripts (pm= paramagnetic impurities), x, y, z, being the fraction of each species (further details in supp. info. of ref. [20]). The fit yields 2J=-196±5 $cm^{-1}$ for the shifted chains and $2J_{intra}=2J_{inter}$=-205±5 $cm^{-1}$ for the spin chain, with x= 0.54, y= 0.45, z= 0.01. The values of the coupling constant are consistent with the value found in the bulk state (2J=-198±5 $cm^{-1}$). The value of g was kept at g= 2.17 as determined independantly by ESR.

The fit therefore indicates that about half of the filaments, or parts of filaments pile up in a different fashion. The origin of this effect in the encapsulated state is still unknown. It is suspected that the chains surrounding the filaments exert some constraint, which eventually modifies the original piling [20]. It is worth emphasizing that such a magnetic effect is usually found in highly organized systems (crystals). Its observation in a gel is probably the first occurrence observed in a randomly-dispersed system.

### *2.3. Sheathing polymer fibrils with self-assembled systems.*

#### 2.3.1. Case of isotactic polystyrene: a neutral polymer.

Recently, Mésini and coworkers have synthesised molecules (bhpb-10 see figure 1) capable of forming nanotubes with very narrow inner and outer radii distributions [24] (figure 8a). The occurrence of these nanotubes is clearly demonstrated by small-angle scattering experiments (figure 8b).

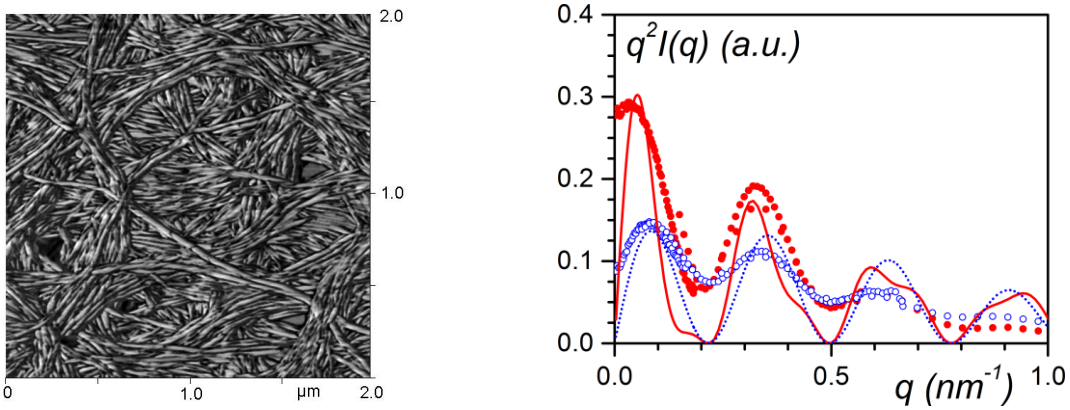


(**a**) (**b**)

**Figure 8.** (a) AFM picture of nanotubes formed in *trans*-decahydronaphthalene (Guenet unpublished data); (b) Scattering curves plotted by means of a Kratky representation $q^2I(q)$ vs q [25]; (●) phbp-10/*trans*-decahydronaphthalene$_D$ system, (○) $iPS_D$/bhpb-10/*trans*-decahydronaphthalene$_D$ hybrid gel. Blue dotted line= fit with equation (5), red solid line= fit with equation (6).

The scattering curve of the bhpb-10/*trans*-decahydronaphthalene$_D$ system can be fitted with a bunch of parrallel hollow cylinders [25]:

$$q^2I(q) = \left[2\pi qC\mu_L\left[\frac{2}{(1-\gamma^2)r_{ext}}\times\{J_1(qr_{ext})-\gamma J_1(q\gamma r_{ext})\}\right]^2\right]\times\sum_{j=1}^{n}\sum_{k=1}^{n}J_o(qr_{jk}) \quad (5)$$

Preprints (www.preprints.org) | NOT PEER-REVIEWED | Posted: 22 March 2018 doi:10.20944/preprints201803.0193.v1

Peer-reviewed version available at Gels 2018, 4, 35; doi:10.3390/gels4020035



The bracketed first term stands for the scattering by a hollow cylinder where $r_{out}$ is the external radius, $\gamma r_{out}$ the value of the inner radius, C the concentration and $\mu_L$ the mass per unit length. J is the Bessel function of first kind with $J_1$ of first order, and $J_0$ of zeroth order. The second term in relation (5) represents intermolecular interactions between pairs of parralel cylinders. Indeed, as can be seen in figure 8a, a large number of nanotubes are parrallel one another, a fact which must be taken into account.

DSC experiments carried out on the hybrid system have suggested the occurrence of a heterogeneous nucleation effect, which is consistent with a sheathing process [25]. AFM investigations have shown an increase of the polymer fibrils cross-ections. These are, however, only circumstancial evidence. Neutron scattering experiments performed by varying the contrast of the different species have allowed one to confirm the sheathing of the polymer fibrils. By using an isotopic solvent mixture that matches the coherent signal of either species (figure 9a), Dasgupta et al have derived the following conclusions [25]:

i) Matching the coherent scattering of deuterated isotactic polystyrene ($iPS_D$) with deuterated *trans*-decahydronaphthalene$_D$ allows one to determine the structure of bhpb-10 molecules in the ternary system. The scattering curve differs from that recorded in the binary system (figure 8b) as it can still be fitted with a hollow cylinder model yet without considering intermolecular terms. This means that parrallel cylinders are absent as would be the case if the nanotubes were randomly oriented through the sheathing process (see figure 9a).

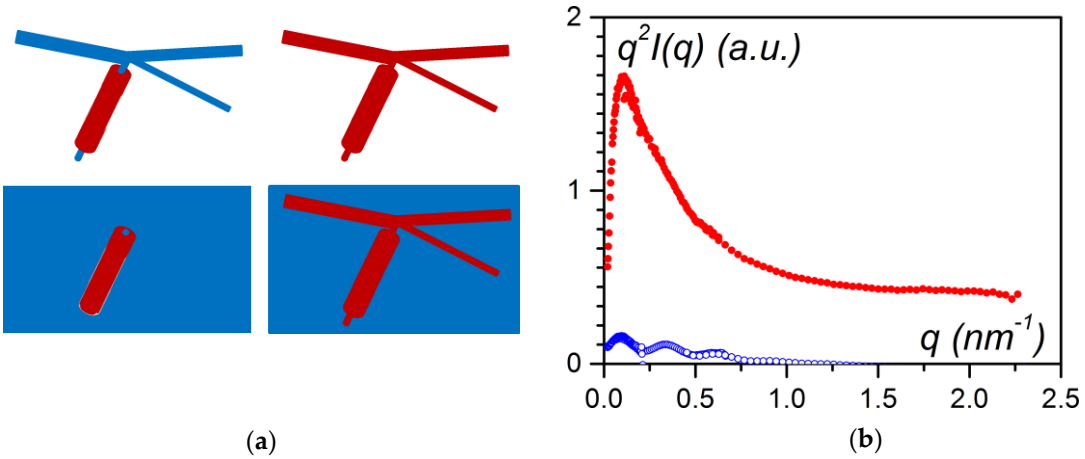


**Figure 9.** (a) sketch of nanotubes sheathing polymer fibrils. The nanotubes are there randomly oriented. The colours stand for hydrogenous species (red) and deuterated species (blue) for illustrating the contrast matching. In a deuterated solvent (blue) only the hydrogeneous species are seen. (b) scattering curves for $iPS_D$/bhpb-10/*trans*-decahydronaphthalene$_D$ (○) and $iPS_H$/bhpb-10/*trans*-decahydronaphthalene$_D$ (●) plotted by means of a Kratky representation $q^2I(q)$ vs q [25].

ii) when hydrogeneous iPS is used instead of deuterated iPS the oscillations previously observed disappear (figure 9b). Here iPS and bhpb-10 have virtually the same scattering amplitude so that they cannot be distinguished any longer. There is an absence of oscillations which is explained through the sketch of figure 9a. Due to their well-defined inner diameter bhpb-10 nanotubes can only sheathe those fibrils with adequate cross-sections; as there is a large cross-section dispersity [21] oscillations are damped and eventually totally vanish. If the nanotubes were independent of the polymer structure, oscillations would superimpose onto the iPS scattering.

The neutron scattering experiments together with the contrast matching give direct evidence that nanotubes do sheathe a fraction of the polymer fibrils. The mechanism involved in the sheathing process is most probably the hetergeneous nucleation of the nanotubes by the polymer fibrils.

### 2.3.2. Case of P3BT (Poly[3-butylthiophene-2,5-diyl]): a semi-conducting polymer.

The case of iPS fibrils sheathed by nanotubes has been useful for establishing a proof of concept,

Preprints (www.preprints.org) | NOT PEER-REVIEWED | Posted: 22 March 2018 doi:10.20944/preprints201803.0193.v1

Peer-reviewed version available at Gels 2018, 4, 35; doi:10.3390/gels4020035



but applications are not in view for such a system. Conversely, sheathing semi-conducting polymers, thus allowing one to prepare semi-conducting nanowires, seems a more promising perspective in the field of functional materials. Exploring new paths in the processing of these polymers may offer new opportunities for application purposes.

Raj, Boulaoued and coworkers [26] studied the possibility of sheathing fibrils of P3BT (Poly[3-butylthiophene-2,5-diyl] figure 10a) which well-known in the organic electronics as p-type materials [27].

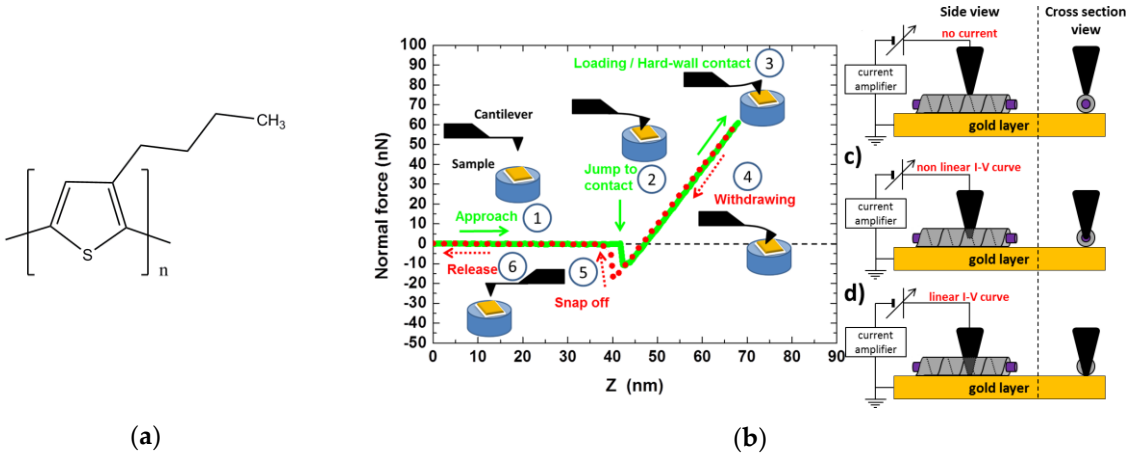


(a) (b)

**Figure 10.** (a) chemical structure of P3BT. (b) right: the tip of the C-AFM is gradually allowed to penetrate into the selected fibril until it reaches the gold layer. The current and the force are simultaneously measured to determine the conductivity and the penetration depth, respectively (for details see reference [26]). Copyright 2018 John Wiley & Sons.

As P3BT fibril grow somewhat slowly, the preparation procedure of the hybrid system involves three steps: first, the P3BT fibres are allowed to grow for several hours at room temperature, second the system is heated up at 60°C and then a bhpb-10 solution is added at the same temperature (no nanotubes are formed at this temperature), third the mixture is cooled down to room temperature for triggering the formation of nanotubes.

Two different types of investigations are then performed: conducting AFM (C-AFM) on dilute solutions, and SANS on more concentrated solutions.

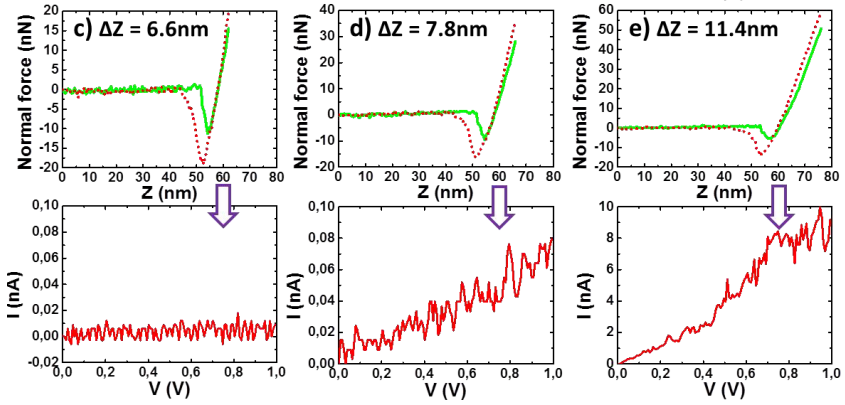


**Figure 11.** I-V plots (lower curves) vs penetration depth (upper curves). From left to right: insulator behaviour, appearance of current, semi-condutor behaviour. [26]. Copyright 2018 John Wiley & Sons.

The principle of C-AFM is shown in figure 10b. Once a supposedly-sheathed fibril is spotted, the tip of the C-AFM is allowed to penetrate gradually into it while the current is measured (intensity vs voltage, I-V curve). The distance Z after the “jump to contact" is the sum of cantilever deflection and of the tip penetration/indentation depth (see figure 10b). Figure 11 shows that the tip first encounters an isolating layer until it reaches a certain depth where the I-V curve corresponds to

Preprints (www.preprints.org) | NOT PEER-REVIEWED | Posted: 22 March 2018 doi:10.20944/preprints201803.0193.v1

Peer-reviewed version available at Gels 2018, 4, 35; doi:10.3390/gels4020035



a semi-conducting system. This result gives a strong indication of P3BT fibrils being sheathed by bhpb-10 nanotubes.

Another experiment was carried out by mapping the current that flows across grounded and isolated gold electrodes separated by an insulating 5 μm trough [26]. By using contact mode C-AFM, current maps are concomitantly recorded with the topography. When pure bhpb-10 is deposited between the electrodes no current is detected in the trough nor in the isolated electrode. When P3BT fibrils are deposited, current is detected in the trough and in the isolated electrode. When the the hybrid system is deposited no current is detected in the trough while current is measured on the isolated electrode. This gives a strong indication of the existence of nanotube-sheathed P3BT fibrils that can be described as insulated molecular wires (see inset of figure 12a).

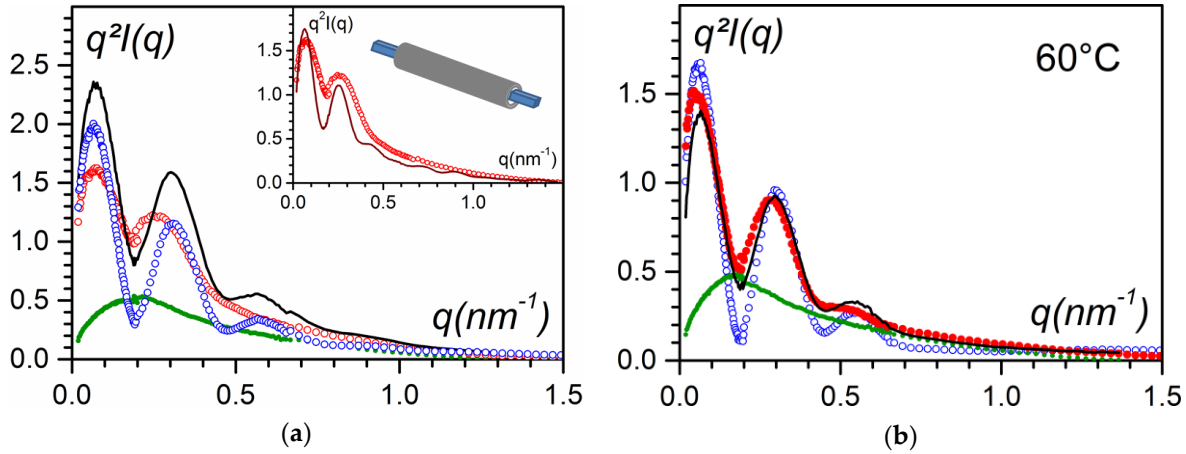


**Figure 12.** SANS curves plotted by means of a Kratky-plot, $q^2I(q)$ vs q. For both figures: ○= bhpb-10/*trans*-decahydronaphthalene; ○= hybrid system; ●= P3BT fibrils in *trans*-decahydronaphthalene; solid black line= sum of the scattering curves of the binary systems (●+○). (a) results obtained at T= 20°C, inset fit of the scattering curve of the hybrid system with the model shown (blue= P3BT fibrils, grey= nanotube; see text for details). (b) results at 60°C [26].

SANS experiments bring additional back up to the sheathing process. P3BT are known to form fibrils of rectangular cross-sections [28,29], which is confirmed by a fit of the scattering curve with [30]:

$$q^2I(q) \sim \frac{2q\mu_L}{\pi}\int_o^{\pi/2}\left[\frac{sinqa/2cos\theta}{qa/2cos\theta}\times\frac{sinqb/2sin\theta}{qb/2sin\theta}\right]^2 sin\theta d\theta \quad (6)$$

which yields a= 4 nm and b= 14 nm, corresponding to a diagonal of about 15 nm.

Figure 12a shows that the scattering curve of the hybrid system differs from the simple sum of the scattering curves of the P3BT fibrils and of the bhpb-10. Clearly, the ternary system is not a mixture of P3BT fibrils and bhpb-10 nanotubes.

Conversely, at 60°C , the scattered intensity of the ternary system is now the sum of the scattered intensity of each component in the binary systems scaled by a factor 0.7. This means that the hybrid entity observed at lower temperature represented about 30% of the components.

In the inset of figure 12a a tentative fit is perfomed considering nanotubes sheathing the P3BT fibrils by using the following relation:

$$I^{theo}_{hybrid}(q) \sim \frac{\pi\mu_{LHyb}}{q}\left[\frac{2\gamma A_{P3BT}}{A_m q r_{out}}J_1(q\gamma r_{out}) + \frac{2A_{bhpb-10}}{A_m q r_{out}}\times\left(J_1(qr_{out}) - \gamma J_1(\gamma q r_{out})\right)\right]^2 \quad (7)$$

where $A_{P3BT}$ and $A_{bhpb-10}$ are the scattering amplitude of the P3BT moiety and of the bhpb-10 molecules, with $A_m = \gamma^2 A_{P3BT} + (1-\gamma^2)A_{bhpb-10}$, $r_{out}$ the outer radius of the hybrid system (namely the sheathing nanotubes), and $\gamma r_{out}$ the inner radius of the sheathing nanotube Considering that there is only 30% of the hybrid system here, the intensity should be written:

$$I(q) = 0.35 \times I^{exp}_{P3BT}(q) + 0.35 \times I^{exp}_{BHPB-10}(q) + 0.3 \times I^{theo}_{hybrid}(q) \quad (8)$$

Preprints (www.preprints.org) | NOT PEER-REVIEWED | Posted: 22 March 2018 doi:10.20944/preprints201803.0193.v1

Peer-reviewed version available at Gels 2018, 4, 35; doi:10.3390/gels4020035



The major goal in the fiting procedure is to match the positions of the first two maximum Under these conditions one obtains $r_{out}$= 20 nm and $\gamma r_{out}$ = 9 nm with a relatively good agreement with the magnitude of the intensity. The inner radius is consistent with the half-value of the diagonal of the P3BT ribbons (7.5 nm). The outer radius is about 1.6 larger than the outer radius of the pure nanotubes, which gives a layer of about 11 nm, a value in agreement with the outcomes of the C-AFM data.

The C-AFM outcomes suggest that most of the P3BT fibrils are sheathed while only 30% of hybrid material need be considered to account for neutron scattering results. This might be due to the fact that the concentration domains differ by about two order of magnitude. Also, the hybrid material has disappeared at 60°C while P3BT fibrils and bhpb-10 nanotubes are still present. That the hybrid system melts at lower temperature is reminiscent of the behaviour of an eutectic compound. This further backs up the occurrence of the sheathing process as an eutectic compound requires an intimate mixture of two components.

### 2.3.3. Case syndiotactic polystyrene with a partially-fluorinated self-assembled system.

Another system involving a partially-fluorinated bhpb-10 (designated as bhpbf, see figure 13b) and syndiotactic polystyrene (sPS) was investigated by Khan et al. with the aim of preparing highly hydrophobic materials. While the expected target was not reached, nanohybrid materials were still obtained [31]. Unlike bhpb-10 bhpbf does not form nanotubes but twisted helices instead where the fluorinated moiety is located in their core [32].

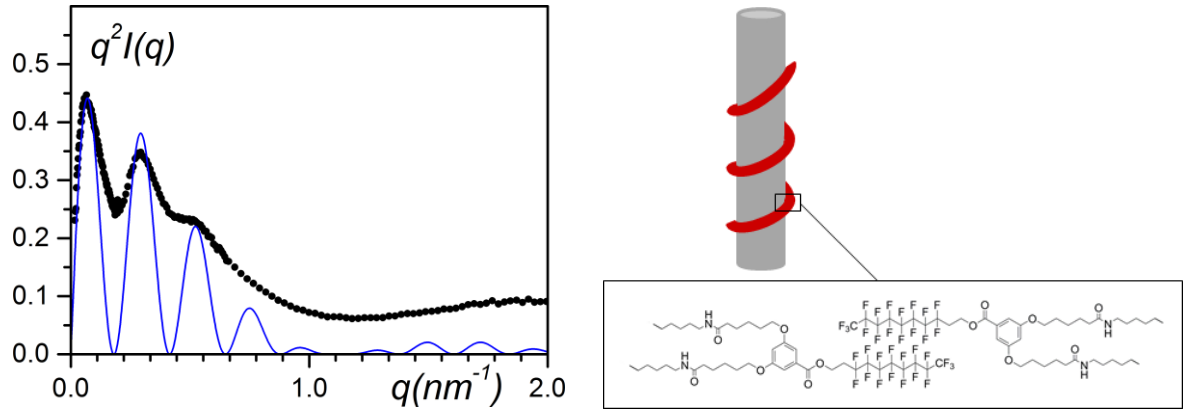


(**a**) (**b**)

**Figure 13.** (a) SANS data plotted by means of a Kratky-plot, $q^2I(q)$ vs q.; ●= sPSD/bhpbfH/o-xyleneD ($C_{bhpbfH}$ = 0.01 g/cm3, $C_{sPSD}$ = 0.15 g/cm3); solid line= fit with equation (9). (b) model designated as "bindweed", where bhpbf irregular helices wind up around polymer fibrils [31].

Among the various types of experiments performed for determining the structure of the hybrid system, results from neutron scattering data are worth mentioning. The system is prepared from deuterated syntiotactic polystyrene ($sPS_D$), hydrogeneous bhpbf and deuterated *p*-xylene so that the main contribution is due to the bhpbf moiety. Khan et al. have shown that the intensity can be fitted with the equation of a hollow cylinder [32]:

$$q^2I(q) = 2\pi qC\mu_L \left[\frac{2}{(1-\gamma^2)r_{ext}} \times \{J_1(qr_{ext}) - \gamma J_1(q\gamma r_{ext})\}\right]^2 \quad (9)$$

where $r_{ext}$ is the external radius, the other parameters being the same as the previous equations.

This points towards an irregular helical structure winding up around the polymer fibrils (the bindweed model) as the derived mass per unit length, $\mu_L \approx 2 \times 10^3$ g/mol.nm, is not consistent with a nanotube for which one would get $\mu_L \approx 3.4 \times 10^5$ g/mol.nm. Again, because of the low resolution in the explored q-range, a helical structure, regular or irregular, scatters like a hollow cylinder (it corresponds to the zeroth order layer line). Here too, the fitting procedure consists in matching

above all the position of the maxima of the oscillations, which yields $r_{ext}$ = 16 nm with $\gamma$ = 0.65. Also the fit allows one to reproduce closely the scattering envelop. The fit could certainly be improved by taking into account radius dispersity. The thickness $\delta$ of the helical structure, namely $\delta = r_{ext} - \gamma r_{ext}$= 5.6 nm is in agreement with the helical parameters of bhpbf reported earlier [32], which gives further support to the validity of the fitting procedure.

Note that the polymer fibrils are basically sheathed the same way by the self assembling molecules whether these are intrinsically forming nanotubes (bhpb-10) or not (bhpbf). To some extent the irregular helix of bhpbf could be regared as an open nanotube.

## 3. Conclusions

This short review highlights the possibility of preparing a large variety of hybrid systems from covalent polymers and self-assembling molecules by simply implementing physical processes such as *heterogeneous nucleation* and *thermoreversible gelation*. This preparation method can be achieved thanks to the high compatibility of the components in the SOL state. By virtue of the intrinsic gel morphology, which consists of an array of randomly-dispersed, thin fibrils, the resulting molecular structures lie typically in the nanometre range. Functional materials can thus be obtained, where the functionality is provided by the self-assembled moiety, and most notably at a relatively-low concentration. Thanks to the nanometre aspect a new, unexpected magnetic property turns out to be imparted to the bicopper complex in the hybrid system. So far, such a magnetic property has been only observed in highly organized systems. In the case of P3BT insulated semi-conducting nanowires can be prepared, again by only using a physical process, which provides one with a novel, unexplored way of processing this polymer.

The examples presented herein may pave the way for preparing functional materials in a rather easy way without resorting to complex chemical synthesis.

**Acknowledgments:** part of the work presented here was funded by ANR (French national research agency) under MATISSE grant (ANR-11-BS08-001), the Indo-French Centre for the Promotion of Advanced Research (IFCPAR, project N°3708-2), and CNRS (Centre National de la Recherche Scientifique). The author is indebted to the following colleagues for supervising: 1) EXAFS measurements, J.L. Bantignies; 2) C-AFM measurements, J. Faure-Vincent; 3) nanotubes and bicopper complex syntheses, P. Mésini; 4) OPVOH synthesis, A. Ajayaghosh.

**Conflicts of Interest:** The author declares no conflict of interest. The founding sponsors had no role in the design of the study; in the collection, analyses, or interpretation of data; in the writing of the manuscript, and in the decision to publish the results.

## References


1. Terech, P.; Weiss, R.G. Low molecular mass gelators of organic liquids and the properties of their gels *Chemical Reviews*, **1997**, *97*, 3133-3159
2. Babu, S.S.; Praveen, V.K.; Ajayaghosh, A. Functional π-Gelators and Their Applications, *Chemical Reviews* **2014**, *114*, 1973-2129
3. *Molecular Gels: Materials with Self-Assembled Fibrillar Networks,* eds; Terech, P.; Weiss, R.G., Springer Verlag, New-York, 2006
4. Liu, X.L.; Li, J.L. *Soft Fibrillar Materials: Fabrication and Applications*, Wiley-VCH, Weinheim, 2013
5. Weiss, R.G. The past, present and future of molecular gels. What is the status of the field, and where is it going*? JACS* **2014**, *136*, 7519-7530
6. Guenet, J.M. *Organogels: Thermodynamics, Structure, Solvent Role and Properties*, Springer, New-York, 2016
7. Lehn, J.M. *Supramolecular chemistry: concepts and perspectives*, VCH-Weinheim-N.Y, 1995.
8. Guenet, J.M. *Thermoreversible gels from polymers and biopolymers*, Acad. Press, London, 1992
9. Salé P. (Société Rhodiaceta), Procédé de preparation de solutions de chlorure de polyvinyle et produits en resultant, République Française, Pat No980874, January 1951.
10. Dasgupta, D.; Srinivasan, S.; Rochas, C.; Ajayaghosh, A.; Guenet, J.M. Hybrid thermoreversible gels from covalent polymers and organogels *Langmuir* 2009, *25*, 8593-8598
11. D. Collin and J.M. Guenet, unpublished results
12. Terech, P.; Schaffhauser, V.; Maldivi, P.; Guenet, J. M. Rheological and neutron scattering investigations of the jelly state of binuclear copper complexes in cyclohexane *Europhys. Let.* 1992, *17*, 515-521
13. Dammer, C.; Maldivi, P.; Terech, P.; Guenet, J.M. Rheological Study of a Bicopper Tetra-carboxylate/Decalin Jelly *Langmuir* 1995, *11*, 1500-1506
14. Bleaney, B.; Bowers, K. D. Anomalous Paramagnetism of Copper Acetate. *Proc. R. Soc. Lond. Ser. Math. Phys. Sci.* 1952, *214*, 451–465.
15. Martin, R. L.; Waterman, H. Magnetic Studies with copper(II) Salts. Part II. Anomalous Paramagnetism and δ-Bonding in Anhydrous and Hydrated copper(II)n-Alkanoates. *J. Chem. Soc.* 1957, 2545–2551.
16. Abied, H.; Guillon, D.; Skoulios, A.; Dexpert, H.; Giroud-Godquin, A. M.; Marchon, J. C. Etude Par Spectroscopie EXAFS Au Seuil K Du Cuivre Des Phases Cristallines et Colonnaires Du Stéarate de Cuivre. *J. Phys.* 1988, *49*, 345–352.
17. Lopez, D.; Guenet, J.M. Encapsulation of filaments of a self-assembling bicopper complex in polymer nanowires. *European Phys. J. B* 1999, *B12*, 405-411
18. Lopez, D.; Guenet, J.M. Structure of a self-assembling bicopper complex in organic solvents and in polymer solutions. *Macromolecules* 2001, *34*, 1076-1081;
19. Poux, S.; Thierry, A.; Guenet, J.M. Mixing of a Self-assembled Supramolecular Polymer and a Covalent Polymer in Organic Solutions *Polymer* 2003, *44*, 6251-6257
20. Boulaoued, A. ; Bantignies, J.L. ; Le Parc, R. ; Goze-Bac, C. ; Mesini, P. ; Nguyen, T.T.T. ; Al Ouahabi, A. ; Lutz, P. ; Guenet, J.M. Hybrid fibrillar xerogel with unusual magnetic properties *Langmuir* **2016**, *32*, 13193-13199
21. Guenet, J.M. Scattering by prolate, cross-section polydispersed cylinders applicable to fibrillar thermoreversible gels *J. Phys. II (Paris)* 1994, *4*, 1077-1082
22. Guenet, J.M.; Poux, S.; Lopez, D. Thierry, A.; Mathis, A.; Green, M.M.; Liu, W. Encapsulation of Magnetic Self-assembled Systems in Thermoreversible Gels *Macromol. Symp*. 2003, *200*, 9-19
23. Sayers, D.E.; Stern, E.A.; Lytle, F.W. New Technique for Investigating Noncrystalline Structures: Fourier Analysis of the Extended X-Ray—Absorption Fine Structure, *Phys. Rev. Lett.* 1971, *27*, 1204–1207.
24. Díaz, N.; Simon, F.-X.; Schmutz, M.; Rawiso, M.; Decher, G.; Jestin, J.; Mésini, P.M. Self-Assembled Diamide Nanotubes in Organic Solvents *Angew. Chem., Int. Ed. Engl.* 2005, *44*, 3260-3264.
25. Dasgupta, D. ; Kamar, Z.; Rochas, C. ; Dahmani, M. ; Mesini, P.J.; Guenet, J.M. Design of hybrid networks by sheathing polymer fibrils with self-assembled nanotubules *Soft Matter* 2010, *6*, 3576
26. Raj, G.; Boulaoued, A.; Lacava, J.; Biniek, L.; Mésini, P.J.; Brinkmann, M.; Faure-Vincent, J.; Guenet, J.-M. Insulated Molecular Wires: Sheathing Semiconducting Polymers with Organic Nanotubes through heterogeneous Nucleation *Adv. Electron. Mater*. 2017, *3*, 1600370
27. Ewbank, P.C.; Stefan, M.C.; Sauve, G.; McCullough, R.D. in *Handbook of Thiophene-Based Materials: Applications in Organic Electronics and Photonics*, Vol 1, Eds. I. F. Perepichka, D. F. Perepichka, John Wiley & Sons Ltd, West Sussex, UK 2009, pp. 157–203.

28. Berson, S.; De Bettignies, R.; Bailly, S.; Guillerez, S. Poly(3-hexylthiophene) Fibers for Photovoltaic Applications *Adv. Funct. Mater*. 2007, *17*, 1377
29. Jo, S.B.; Lee, W.H.; Qiu, L.; Cho, K. Polymer blends with semiconducting nanowires for organic electronics *J. Mater. Chem*. 2012, *22*, 4244.
30. Mittelbach, P., Porod G. Zur Röntgenkleinwinkelstreuung verdünnter kolloiden Systeme *Acta Physica Austriaca*, 1961, *14*, 185-211
31. Khan, A.N.; Schmutz, M.; Lacava, J.; Al Ouahabi, A.; Nguyen, T.T.T.; Mesini, P.J.; Guenet, J.-M. Design of Nanohybrid Systems from a Partially Fluorinated Organogelator and Syndiotactic Polystyrene thermoreversible Gel *Langmuir* 2015, *31*, 7666−7672
32. Khan, A.N.; Nguyen, T.T.T.; Dobircau, L.; Schmutz, M.; Mesini, P.J.; Guenet, J.-M. An investigation into the interactions involved in the formation of nanotubes from organogelators *Langmuir* 2013, *29*, 16127-16134